A Pockels cell enabled heterodyne Phase Contrast Imaging diagnostic for detection of Ion Cyclotron Emission

A. Marinoni,[1, a)] C.P. Moeller,[2] J.C. Rost,[1] M. Porkolab,[1] and E.M. Edlund[1, b)]

[1)] *Plasma Science and Fusion Center, Massachusetts Institute of Technology, Cambridge (MA) 02139, USA*

[2)] *General Atomics, San Diego (CA) 92121, USA*

(Dated: 8 August 2022)

This work describes a novel optical heterodyne detection scheme that significantly extends the frequency response of the Phase Contrast Imaging (PCI) method to detect electron density fluctuations in tens of megahertz frequency range. The system employs a variable frequency electro-optic modulator to allow operation at any frequency in the range 10–40 MHz without the need to re-align the system. The frequency coverage of the system makes it suitable to measure the radial structure of the electron density component of Ion Cyclotron Emission on devices having confining magnetic field of a few Tesla, thus extending the purely temporal measurements provided so far by magnetic probes.

[a)] marinoni@mit.edu

[b)] Present address: SUNY Cortland, Cortland (NY) 13045, USA

I. INTRODUCTION

Understanding the propagation of waves in magnetically confined plasmas is a broad and complex topic that has been the subject of intense theoretical and experimental investigations for nearly a century. Its extent can be appreciated by noting that oscillations span several orders of magnitude both in frequency, from kHz to hundreds of GHz, and spatial scales, from the electron gyro-radius to the size of the plasma itself, either as turbulent or coherent phenomena. The experimental characterization of the entire spectrum of waves is an extremely challenging task due to constraints in the measurements; such limitations can be of a technological nature, e.g. inadequate signal to noise ratio or spatio-temporal response of the apparatus in use, or due to the inability to detect a given component of the wave under consideration. In this work we expose a method to detect the spatio-temporal characteristics of a particular class of instabilities in the cyclotron range of frequencies, commonly referred to Ion Cyclotron Emission (ICE). First predicted in the 1950s[1–4], this class of waves is believed to be a Compressional Alfvén Eigenmode generated by anisotropies, or inversions, in the distribution function of energetic particles that causes emission of electromagnetic radiation in bands centered around the thermal ion cyclotron frequency, as well as higher harmonics[5]. While ICE was first observed in the late 1970s on the TFR tokamak[6], it sparked increasing interest in the fusion community only from the early 1990s thanks to its suitability as a passive diagnostic tool of the energetic ion population that is compatible with the harsh environment in future fusion reactors. As such, it was searched for and observed on many magnetically confined plasma devices[7–17] which detected emission caused by either supra thermal beam ions or fusion products. Although there exist numerous measurements of frequency spectra and toroidal mode numbers, the radial and poloidal structures of the instability are still elusive because all the reported measurements were performed using either external magnetic loops or heating antennas operated in receiving mode, both of which are not capable of directly measuring the RF field components in the plasma core. Additionally, diagnostic systems that are usually employed to detect the radial or poloidal structure of a given instability cannot detect ICE because its frequency exceeds the diagnostic bandwidth. The system described in this work was conceived to fill this gap and provide further constraints to the theoretical description of the instability which is not yet complete, especially in the non-linear phase[18].

The paper is organized as follows: Section II gives an overview of the Phase Contrast Imaging method; the technical details of the heterodyne PCI for ICE detection are described in Section III; conclusions are offered at the end.

II. THE PHASE CONTRAST IMAGING METHOD

The Phase Contrast Imaging (PCI) method is an optical technique that uses probing light traveling through a transparent medium, and converts phase shifts induced on the probing wavefront into amplitude variations at the image plane. Invented in the 1930s by F. Zernike[19], who proved its superior sensitivity compared to competing methods used in cellular microscopy, its application to plasmas was pioneered by M. Presby and D. Finkelstein in the late 1960s[20] while H. Weisen ported it to fusion grade plasmas to measure fluctuations associated with plasma turbulence and radio frequency driven waves on the TCA tokamak in the late 1980s[21]. In very simplistic terms, the PCI technique can be described as an internal reference interferometer, i.e. for which both legs travel through the plasma, that measures the spatial distribution of electron density fluctuations by imaging the probing laser beam onto an array of detectors. More specifically, for fluctuations with wavelengths of a few mm to a few cm, which are typically active in modern fusion devices, and at the probing wavelength of 10.6 µm, which is commonly used by PCI systems worldwide, diffraction occurs in the Raman-Nath rather than in the Bragg regime[22]. In such conditions, the plasma behaves as a transparent object in which phase shifts caused by the plasma are small, usually below milli-radians levels, and are given by

$$\phi(\mathbf{x}_\perp, t) = \lambda_0 r_e \int_a^b dx_\parallel \; n_e(\mathbf{x}, t), \tag{1}$$

where r_e is the classical electron radius, n_e is the plasma electron density, the parallel spatial coordinate refers to the propagation direction of a probing laser beam of vacuum wavelength λ_0 between two generic locations denoted as a and b. The total phase shift, ϕ, is usually decomposed into a component given by the stationary plasma density, $\phi_0(\mathbf{x}_\perp)$, and that due to fluctuations, $\tilde{\phi}(\mathbf{x}_\perp, t)$, which is usually much smaller than the former. The heart of the technique consists of separating the two legs in a focal plane of the optical system where, by using a custom component called *phase plate*, a $\pi/2$ phase shift is induced thanks to a groove of suitable depth (see Fig.6 in[20]). As a result, the total electric field, E_{tot}, of the

probing wave is expanded to first order into

$$E_{tot}(\mathbf{x}_\perp, t) = E_0 e^{\imath\phi(\mathbf{x}_\perp, t)} \simeq E_{\phi_0}[1 + \imath\tilde{\phi}(\mathbf{x}, t)], \tag{2}$$

where spatial dependencies of the stationary plasma density and of the probing electric field have been omitted for simplicity. Equation 2 states that the total electric field, E_{tot}, is composed of the reference leg field that has interacted with the stationary plasma density, E_{ϕ_0}, plus that of the measurement leg that has interacted with the fluctuating plasma density, $E_{\phi_0}\imath\tilde{\phi}$. The PCI method employs the scattering angles at which the measurement and the reference beams propagate with respect to each other, and separates these two components in a suitable focal plane of the imaging system, where an additional $\pi/2$ phase shift is induced. Additionally, in order to increase the contrast between the two components, the intensity of the reference beam is usually attenuated by a factor $\rho < 1$. The *invisible* phase shifts are thereby made *detectable* as variations in brightness, I, according to the relation

$$I(\mathbf{x}_\perp, t) \simeq I_{\phi_0}[\rho + 2\tilde{\phi}(\mathbf{x}_\perp, t)]. \tag{3}$$

Equation 3 shows that the sensitivity of a PCI system is a factor $2/\rho$ that of a comparable standard homodyne interferometer operated in optimal detection mode (i.e. with the two legs exactly out of phase), with other parameters being equal. Furthermore, the PCI method is insensitive to phase shifts induced vibrations as long as proper optical alignment is maintained, i.e. the phase plate induced $\pi/2$ phase shift is applied.

A. Heterodyning PCI methods

The PCI method is particularly attractive in the field of experimental plasma turbulence because it images fluctuations onto linear or two-dimensional arrays of detectors, thereby making the extraction of spatio-temporal spectra feasible. In order to exploit the extreme sensitivity of the PCI method, detector noise is minimized via cryogenic cooling which, as a drawback, reduces the frequency response of the detectors. As a result, worldwide PCI systems typically use Photo-Conductive or Photo-Voltaic detectors whose 3dB points are within 1 MHz and 10 MHz, respectively. Although suitable for broadband turbulence and low frequency waves, such narrow bandwidths preclude the study of faster phenomena, whose detection requires the use of suitable heterodyning techniques. By modulating the

intensity of the probing laser beam at a frequency close to that of the wave of interest the heterodyne beat frequency falls within the PCI detector bandwidth, thus making the imaging method applicable at higher frequencies. Such technique was used on the Alcator C-Mod tokamak to detect for the first time mode converted Ion Cyclotron slow waves[23] and, by employing the absolute calibration of the PCI system, yielded the first quantitative experimental validation of full-wave models[24]. On the heterodyne PCI system installed on Alcator C-Mod, modulation of the intensity of the laser beam was obtained using acousto-optic modulators (AOMs), which consist of a crystal in which a piezoelectric transducer, driven by an appropriate electric field, excites the propagation of an acoustic wave. The crystal then behaves as a time varying, periodic, diffraction grating which scatters incoming light at the Bragg angle and shifts it in frequency by that of the sound wave. The required intensity modulation of the incoming light is obtained by subsequently recombining the scattered and unscattered components. This method, although successfully used on Alcator C-Mod to detect signals of a given frequency induced by an RF antenna, would not be optimal in case the modulation frequency had to be varied. Indeed, since AOMs typically operate within a narrow bandwidth, of the order of a few MHz, around the frequency of the acoustic wave, the overall modulation frequency can only be varied by combining multiple AOMs. As a consequence, the system has to be realigned every time the modulation frequency is altered; additionally, the overal complexity and the real estate occupied on the optics table rapidly increase with the number of AOMs used. ICE is typically observed over several harmonics spaced by the cyclotron frequency which, on the majority of present fusion devices, can be continuously varied by altering the intensity of the confining magnetic field. As such, it is apparent how the ability to modify the modulation frequency of the heterodyne system is of paramount importance to ICE detection. In view of the above, it was decided to employ an electro-optic modulator (EOM) because this offers continuously variable modulation from DC to GHz bandwidth without altering the beam path of the probing light. The PCI system can be thus be used in heterodyne mode at any available frequency, while standard homodyne operation mode for broadband turbulence detection is recovered by simply turning off the EOM driver.

III. TECHNICAL IMPLEMENTATION

A. Pockels cell

The typical set-up of an EOM consists of a Pockels cell located between two crossed polarizers, i.e. oriented at 90 degrees with respect to each other. The desired amplitude modulation is obtained by the second polarizer projecting the time varying polarization induced by the Pockels cell onto its transmission axis. For light at 10.6 µm it is necessary to use birefringent crystals that belong to the symmetry group $\bar{4}3m$, for which the magnitude of the electro-optic coefficient is such that Pockels cells must be used in a transverse configuration. In this case the normal axes $(\hat{X}, \hat{Y})$ of the crystal are orthogonal to each other and rotated by 45 degrees with respect to the direction of the externally applied electric field. The polarization modulation is obtained when the probing light is linearly polarized at an angle with respect to the normal axis of the crystal[25], so as to induce a phase delay only along the component projected onto the slow axis. In the case of light linearly polarized along the $\hat{y}$ direction, i.e. $\mathbf{E}(\omega t) = E_0 \hat{y} e^{\imath\omega t}$, the electric field at the exit of the crystal of length L reads

$$\begin{aligned} \mathbf{E}(L,t) &= \left(E_X \hat{X} + E_Y \hat{Y} e^{\imath\delta}\right) e^{\imath(k_0 nL - \omega t)} \\ &= \frac{E_0}{2}\left[\left(1 - e^{\imath\delta}\right)\hat{x} + \left(1 + e^{\imath\delta}\right)\hat{y}\right] e^{\imath(k_0 nL - \omega t)}, \end{aligned} \tag{4}$$

where ω is the angular frequency of the probing light, k_0 its wave vector in vacuum, n the refraction index of the crystal at the wavelength of the probing light and δ the induced phase shift. For the case under consideration $\delta = 0.5 k_0 r_{41} n^3 L E_{ext}$, where E_{ext} is the magnitude of the electric field applied to the crystal and r_{41} its electro-optic coefficient. The ratio of the transmitted to incident power is obtained by projecting Eq. 4 along the transmissive axis of the second polarizer and squaring to obtain

$$T = \sin\left(\delta/2\right)^2 = 0.5\left[1 - \cos(\delta)\right]. \tag{5}$$

By orienting the polarizer along $\hat{y}$, the transmissivity is shifted by $\pi/2$ to become $T = \cos(\delta/2)^2 = 0.5[\cos(\delta) - 1]$, while it does not depend on the externally applied electric field when the polarizer is rotated 45 degrees with respect to $\hat{x}$ (all such properties were verified during system testing). The system was tested on a bench-top depicted in Fig. 1, from which it can be noted that the laser (Diamond C-20, from Coherent inc., USA) provides

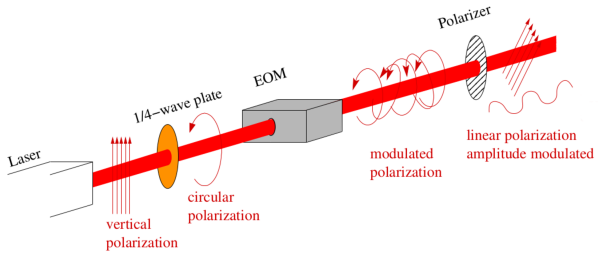

FIG. 1. Conceptual layout of an EOM with $\lambda/4$ wave-plate.

light that is already linearly polarized, and that a quarter-wave plate (WPM-10.6 from II-VI, USA) is located before the exit polarizer. Light was detected using a GHz bandwidth single element detector (UHSM-10.6 from Vigo, Poland). The quarter-wave plate is used to increase the modulation depth when the applied electric field is smaller than that resulting in $\delta = \pi$. Indeed, by applying a quarter-wave difference between the ordinary and extraordinary components of the probing light Eq. 5 becomes

$$T = \sin(\delta/2 + \pi/4)^2 = 0.5[1 + \sin(\delta)]. \tag{6}$$

During system testing, it was found that by moving the quarter-wave plate from upstream to downstream of the Pockels cell, the modulation depth increased by approximately 10%, possibly due to the laser beam being not perfectly polarized along the vertical direction. The birefringent crystal is shaped as a regular parallelepiped with dimensions 5x5 mm^2 and 5 cm, respectively, across and along the propagation direction of the laser beam. The crystal dimensions were chosen in such a way as to maximize the phase shift δ while maintaining the cross section large enough for the crystal not to become structurally too fragile. Indeed, the cross-sectional dimension is a compromise between the need to accommodate a collimated laser beam of finite size while not requiring too large of a voltage for a given intensity of the external electric field which, for a given crystal length, determines the magnitude of the phase shift. Finally, cost considerations apply to the total volume of the crystal. The crystal is water cooled for thermal stability and cut along the Miller indices that maximize the phase shift δ, other quantities being equal[25]. More specifically, the cross section is oriented along directions (110), gold coated electrodes are applied on the surface $(1\bar{1}0)$, while the water cooled surfaces are in contact with surface (001). The crystal was chosen to be CdTe because, among birefringent materials suited for light at 10.6 µm wavelength, it features the largest electro-optic coefficient thereby lowering the voltage requirements for a given crystal size.

More specifically, for the case of the crystal and the optical set-up used in this work, 100% modulation depth is theoretically obtained with sinusoidal amplitude of 2217 V, as opposed to 3410 V for ZnTe, 4926 V for GaAs and 8867 V for ZnSe. The CdTe crystal and the water cooling enclosure were commissioned to II-VI inc. The enclosure, made of anodized aluminum, was later modified to reduce RF leakage by adding an additional ground path and further enclosing it with a standard 6061 Al box. The total size of the enclosure is 10x10x7 cm^3. Eq. 6 models the adiabatic approximation of a Pockels cell, i.e. the limit in which the time required by photons to travel along the crystal is negligible compared to the modulation frequency. It can be shown that, by accounting for the fact that the probing light demodulates when the voltage changes sign during the transit time, the phase delay δ reduces by the quantity $\rho = |\sin(\pi f\tau)/(\pi f\tau)|$, where f the modulation frequency and τ is the time required by photons to travel through the crystal[26]. For the system in use the non-adiabatic effect is negligible as the attenuating factor ρ is equal to about 99.9%. In a purely capacitive component such as a Pockels cell, dielectric losses are the primary cause of power dissipation and, therefore, determine the minimum power to be removed by the cooling system and provided by the RF driver. In the case of a dielectric subject to a sinusoidal electric field, it can be shown[27] that the power per unit volume dissipated in the dielectric is equal to

$$\frac{dP_{loss}}{dV} = \frac{1}{2}\omega\epsilon'_d(\omega)\tan(\theta)|E_{ext}|^2, \tag{7}$$

where ω is the modulation angular frequency, ϵ'_d is the real part of the permittivity and $\tan(\theta)$ is a parameter known as *loss tangent*. Detailed measurements of the loss tangent for CdTe are not readily available in the literature; however, interpolation over existing data indicates that, for the frequency range considered in this work, dielectric losses should not exceed 1 W, thereby making heat removal not problematic. Testing proved that no overheating of the Pockels cell or signal distortion is generated in this frequency range.

B. Voltage driver

In the optical set-up described by Eq. 6, when the externally applied voltage varies in time sinusoidally, the intensity modulation produced by a crystal subject will contain higher order harmonics. Indeed, by using the Jacobi-Anger expansion formula, it can be seen that the strength of each higher harmonic is proportional to the corresponding Bessel function

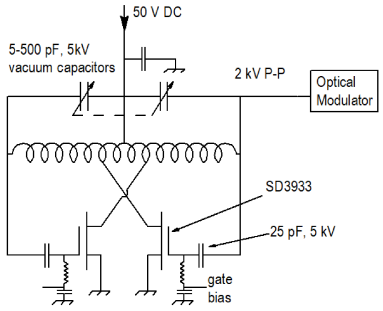

FIG. 2. Reduced diagram of the variable frequency high voltage oscillator.

of the first kind. By imposing that the amplitude of all spurious component in the intensity of the modulated beam be at most one-hundredth of that at the fundamental frequency, one obtains that the modulation depth cannot exceed 50%, or one-third the quarter-wave voltage. It was verified with a spectrum analyzer that higher harmonics are at least 24 dB below the peak corresponding to the fundamental modulation frequency. The presence of higher order harmonics represents an appreciable issue for the detection of fluctuations over extended bandwidth, such as ICE, because higher harmonics might happen to beat with actual waves oscillating at similar frequency, thereby producing a low-frequency signal within the detector bandwidth that could bias the analysis. In case a 100% modulation depth was required, e.g. for S/N considerations, one remedy to the higher order harmonics would be to modulate the voltage with a triangular waveform, so that an almost pure sinusoidal intensity modulation would be obtained. In view of the considerations above, the voltage driver was designed to deliver a sinusoidal waveform of 1 kV amplitude. No spurious harmonic is observed above noise level. The principle of operation is that of a tank circuit which resonates in an extended frequency range thanks to two variable capacitors. It operates according to a feed-back loop where the frequency set by the resonator is sampled and amplified by JFET transistors assembled in a crossed coupled capacitors configuration. The circuitry is shown in Fig. 2.

C. Expected PCI system response

The signal to noise ratio of the heterodyne PCI system can be compared to that of its homodyne counterpart by taking into account the signal loss due to additional components and the power modulation. The transmissivity of the Pockels cell with no applied voltage

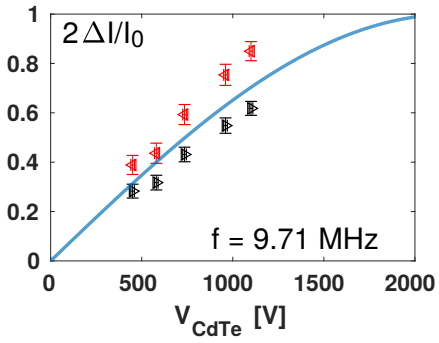

FIG. 3. Modulation depth of the EOM as a function of the voltage amplitude applied to the crystal for a modulation frequency equal to 9.71 MHz. The expected behavior (−) is compared to measurements inferred using the highest (<) and lowest (>) calibration factor of the infrared detector used for testing as declared by the manufacturer.

and that of the quarter wave waveplate was measured to be 98%. The heterodyne detection scheme proposed in this work assumes single side band detection. Although the spatial response properties of the PCI diagnostic are unaffected, the signal-to-noise ratio is reduced. More specifically, we consider probing light intensity of the form $I(t) = \alpha\,[1 + \Delta \sin(\Omega t)]$ where α is the attenuation of the time averaged power and Δ the modulation depth. Compared to homodyne detection, single-band heterodyne detection decreases the signal power by $(\alpha\Delta/2)^2$; noise is reduced by α in case shot noise dominates, while is unaffected in case detector noise dominates. As such, the signal-to-noise ratio decreases by a quantity of the order $\alpha\Delta^2/4$. The laser intensity can be adjusted to compensate for α, following Eq. 6 and Fig. 3 we estimate a reduction of the signal-to-noise ratio up to 90%. Despite this strong reduction, the detection of semi-coherent waves is expected to be feasible given that the PCI features signal a few orders of magnitude above noise level.

IV. CONCLUSIONS

This work describes the design and realization of a heterodyne Phase Contrast Imaging system to detect Ion Cyclotron Emission waves in tokamaks. The system is designed to be employed on the existing PCI diagnostics by modulating the intensity of an infrared laser beam at 10.6 µm wavelength. The modulator is made of a water cooled CdTe Pockels cell driven by a resonant circuit able to generate sinusoidal waveforms up to 2 kV peak-peak, which should guarantee adequate signal-to-noise ratio. The circuit is able to continuously

drive the cell in the frequency region 10–40 MHz.

ACKNOWLEDGMENTS

This work was supported by the US Department of Energy under DE-FG02-94ER54235 and DE-SC0016154.

REFERENCES

[1]K. G. Malmfors, Arkiv Fysik **1**, 569 (1950).

[2]E. P. Gross, "Plasma Oscillations in a Static Magnetic Field," Phys. Rev. **82**, 232–242 (1951).

[3]H. K. Sen, "Solar "Enhanced Radiation" and Plasma Oscillations," Phys. Rev. **88**, 816–822 (1952).

[4]E. G. Harris, "Unstable Plasma Oscillations in a Magnetic Field," Phys. Rev. Lett. **2**, 34–36 (1959).

[5]R. Dendy, C. Lashmore–Davies, and K. Kam, "A possible excitation mechanism for observed superthermal ion cyclotron emission from tokamak plasmas," Physics of Fluids B: Plasma Physics **4**, 3996–4006 (1992).

[6]Equipe-TFR, "High-power neutral injection and ion power balance in TFR," Nuclear Fusion **18**, 1271–1303 (1978).

[7]S. Yamamoto, K. Itoh, A. Fukuyama, and S. Itoh, "Plasma heating by multiple-short-pulse neutral beams," Plasma Physics and Controlled Nuclear Fusion Research **1**, 665 (1984).

[8]G. Cottrell, V. Bhatnagar, O. D. Costa, R. Dendy, J. Jacquinot, K. McClements, D. McCune, M. Nave, P. Smeulders, and D. Start, "Ion cyclotron emission measurements during JET deuterium-tritium experiments," Nuclear Fusion **33**, 1365–1387 (1993).

[9]H. Duong, W. Heidbrink, E. Strait, T. Petrie, R. Lee, R. Moyer, and J. Watkins, "Loss of energetic beam ions during TAE instabilities," Nuclear Fusion **33**, 749–765 (1993).

[10]S. Cauffman, R. Majeski, K. McClements, and R. Dendy, "Alfvenic behaviour of alpha particle driven ion cyclotron emission in TFTR," Nuclear Fusion **35**, 1597–1602 (1995).

[11]M. Ichimura, H. Higaki, S. Kakimoto, Y. Yamaguchi, K. Nemoto, M. Katano, M. Ishikawa, S. Moriyama, and T. Suzuki, "Observation of spontaneously excited waves in the ion cyclotron frequency range on JT-60U," Nuclear Fusion **48**, 035012 (2008).

[12]K. Saito, R. Kumazawa, T. Seki, H. Kasahara, G. Nomura, F. Shimpo, H. Igami, M. Isobe, K. Ogawa, K. Toi, M. Osakabe, M. Nishiura, T. Watanabe, S. Yamamoto, M. Ichimura, and T. Mutoh, "Measurement of Ion Cyclotron Emissions by Using High-Frequency Magnetic Probes in the LHD," Plasma Science and Technology **15**, 209–212 (2013).

[13]S. G. Thatipamula, G. S. Yun, J. Leem, H. K. Park, K. W. Kim, T. Akiyama, and S. G. Lee, "Dynamic spectra of radio frequency bursts associated with edge-localized modes," Plasma Physics and Controlled Fusion **58**, 065003 (2016).

[14]R. Ochoukov, V. Bobkov, B. Chapman, R. Dendy, M. Dunne, H. Faugel, M. García-Muñoz, B. Geiger, P. Hennequin, K. G. McClements, D. Moseev, S. Nielsen, J. Rasmussen, P. Schneider, M. Weiland, and J.-M. Noterdaeme, "Observations of core ion cyclotron emission on ASDEX Upgrade tokamak," Review of Scientific Instruments **89**, 10J101 (2018).

[15]L. Askinazi, A. Belokurov, D. Gin, V. Kornev, S. Lebedev, A. Shevelev, A. Tukachinsky, and N. Zhubr, "Ion cyclotron emission in NBI-heated plasmas in the TUMAN-3M tokamak," Nuclear Fusion **58**, 082003 (2018).

[16]E. D. Fredrickson, N. N. Gorelenkov, R. E. Bell, A. Diallo, B. P. LeBlanc, and M. Podestà, "Emission in the ion cyclotron range of frequencies (ICE) on NSTX and NSTX-U," Physics of Plasmas **26**, 032111 (2019).

[17]K. Thome, D. Pace, R. Pinsker, M. V. Zeeland, W. Heidbrink, and M. Austin, "Central ion cyclotron emission in the DIII-d tokamak," Nuclear Fusion **59**, 086011 (2019).

[18]N. N. Gorelenkov, "Energetic particle-driven compressional alfvén eigenmodes and prospects for ion cyclotron emission studies in fusion plasmas," New Journal of Physics **18**, 105010 (2016).

[19]F. von Zernike, "Beugungstheorie des schneidenver-fahrens und seiner verbesserten form, der phasenkontrastmethode," Physica **1**, 689–704 (1934).

[20]H. M. Presby and D. Finkelstein, "Plasma phasography," Review of Scientific Instruments **38**, 1563–1572 (1967).

[21]H. Weisen, "The phase contrast method as an imaging diagnostic for plasma density fluctuations (invited)," Review of Scientific Instruments **59**, 1544–1549 (1988).

[22]H. Weisen, "The phase-contrast technique as an imaging diagnostic for plasma density fluctuations," Infrared Physics **25**, 543–549 (1985).

[23]E. Nelson-Melby, M. Porkolab, P. T. Bonoli, Y. Lin, A. Mazurenko, and S. J. Wukitch, "Experimental Observations of Mode-Converted Ion Cyclotron Waves in a Tokamak Plasma by Phase Contrast Imaging," Phys. Rev. Lett. **90**, 155004 (2003).

[24]N. Tsujii, M. Porkolab, P. T. Bonoli, E. M. Edlund, P. C. Ennever, Y. Lin, J. C. Wright, S. J. Wukitch, E. F. Jaeger, D. L. Green, and R. W. Harvey, "Validation of full-wave simulations for mode conversion of waves in the ion cyclotron range of frequencies with phase contrast imaging in alcator c-mod," Physics of Plasmas **22**, 082502 (2015).

[25]A. Yariv and P. Yeh, *Optical waves in crystals* (John Wiley & Sons, 1983).

[26]T. A. Maldonado, "Electro-optic Devices," in *The Optics Encyclopedia* (American Cancer Society, 2007) Chap. 13.

[27]A. Marinoni, C. P. Moeller, M. Porkolab, J. C. Rost, E. M. Davis, and E. M. Edlund, "A wide frequency heterodyne detection method using the Pockels effect," Tech. Rep. PSFC/RR-18-3 (Massachusetts Institute of Technology, 2018).